Shoe configuration effects on equine forelimb gait kinetics at a walk

Rita Aoun[1,2], Zaneta Ogunmola[1,2], Anaïs Musso[1], Takashi Taguchi[1,2], Catherine Takawira[1,2] and Mandi J. Lopez[1,2]

[1] Department of Veterinary Clinical Sciences, School of Veterinary Medicine, Louisiana State University and Agricultural and Mechanical College, Baton Rouge, LA, United States of America

[2] Laboratory for Equine and Comparative Orthopedic Research, Department of Veterinary Clinical Sciences, School of Veterinary Medicine, Louisiana State University and Agricultural and Mechanical College, Baton Rouge, LA, United States of America

ABSTRACT

The shift in vertical forces on the equine hoof surface by heart-bar, egg-bar, and wooden clog shoes can significantly impact gait kinetics. Hypotheses tested in this study were that vertical, braking, and propulsion peak force (PF) and impulse (IMP) are different while shod with heart-bar, egg-bar, open-heel, and wooden clog shoes, or while unshod, and the resultant ground reaction force vector ($\mathbf{GRF_{YZ}}$) has the longest duration of cranial angulation with open-heel shoes followed by unshod, then egg-bar and heart-bar shoes, and the shortest with wooden clog shoes. Forelimb GRFs were recorded as six non-lame, light-breed horses walked across a force platform (four trials/side) while unshod or with egg-bar, heart-bar, open-heel, or wooden clog shoes. Outcomes included vertical, braking, and propulsive peak forces (PF_V, PF_B, PF_P) and impulses (IMP_V, IMP_B, IMP_P), percent stance time to each PF, braking to vertical PF ratio (PF_B/PF_V), walking speed (m s^{-1}), total stance time (ST) and percent of stance in braking and propulsion. The magnitude and direction of the resultant $\mathbf{GRF_{YZ}}$ vectors were quantified at 5% stance increments. Kinetic measures were compared among shoeing conditions with a mixed effects model (p-value < 0.05). A random forest classifier algorithm was used to predict shoeing condition from kinetic outcome measures. All results are reported as mean ± SEM. Trial speed, 1.51 ± 0.02 m s^{-1}, was not different among shoeing conditions. The PF_V was lower with wooden clog (6.13 ± 0.1 N kg^{-1}) *versus* egg-bar (6.35 ± 0.1 N kg^{-1}) shoes or unshod (6.32 ± 0.1 N kg^{-1}); the PF_P was higher with wooden clog (0.81 ± 0.03 N kg^{-1}) *versus* open-heel (0.71 ± 0.03 N kg^{-1}) or egg-bar (0.75 ± 0.03 N kg^{-1}) shoes or unshod (0.74 ± 0.03 N kg^{-1}), and lower with open-heel compared to heart-bar shoes (0.77 ± 0.03 N kg^{-1}). Both IMP_B and IMP_V were higher with open-heel shoes (−0.19 ± 0.008 N s kg^{-1}, 3.28 ± 0.09 N s kg^{-1}) *versus* unshod (−0.17 ± 0.008 N s kg^{-1}, 3.16 ± 0.09 N s kg^{-1}), and IMP_V was higher with wooden clog shoes (3.26 ± 0.09 N s kg^{-1}) *versus* unshod. With wooden clog shoes, PF_B/PF_V (0.12 ± 0.004) was higher than unshod (0.11 ± 0.004). Percent time to peak PF_V, PF_B, and PF_P, and percent braking time were highest and percent propulsion time lowest with wooden clog shoes. The magnitude of the $\mathbf{GRF_{YZ}}$ vector with the wooden clog shoe was the highest among shoeing conditions during the first stance half, lowest during the second stance half, highest during late propulsion, and had the most gradual braking to propulsion transition. Vectors were angled cranially with wooden clog shoes slightly longer than the others. Wooden clog shoes was the only shoeing condition accurately predicted from kinetic measures. Distinct, predictable

Submitted 27 August 2024
Accepted 16 January 2025
Published 26 February 2025

Corresponding author
Mandi J. Lopez, mlopez@lsu.edu

Academic editor
Rebecca Parkes

Additional Information and Declarations can be found on page 21

DOI **10.7717/peerj.18940**

Copyright
2025 Aoun et al.

Distributed under
Creative Commons CC-BY 4.0

OPEN ACCESS

How to cite this article Aoun R, Ogunmola Z, Musso A, Taguchi T, Takawira C, Lopez MJ. 2025. Shoe configuration effects on equine forelimb gait kinetics at a walk. *PeerJ* **13**:e18940 http://doi.org/10.7717/peerj.18940

changes in gait kinetics with wooden clog shoes may reduce stresses on hoof structures. Study results enhance knowledge about shoe effects on equine gait kinetics and cutting-edge measures to quantify them.

Subjects Veterinary Medicine, Biomechanics

Keywords Hoof, Horse, Ground reaction force, Wooden clog, Animal biomechanics, Braking, Propulsion, Bar shoes, Forelimb, Force platform

INTRODUCTION

Horseshoes have been employed since the Roman era when "hippo-sandals" were used primarily for protection against rough and abrasive surfaces (*Back & Pille, 2013*; *Karle et al., 2010*; *Lawrence, 1898*). Shoe shape, composition, and affixation techniques have advanced with customization for protection, performance, and therapy. Mechanisms to alleviate limb pain and stabilize and shield hooves compromised by injury or disease continue to evolve with technology, metallurgy, and experience (*Back & Pille, 2013*; *Butler Jr, 1985*; *Clarke et al., 2021*; *Goetz & Comstock, 1985*; *Karle et al., 2010*). Commonly, shoes are designed to alter force distribution over the solar hoof surface, often for targeted stress reduction (*O'Grady, 2017*; *Parks, 2012*; *Van Heel et al., 2005*). However, changes in hoof force distribution during a step cycle can also significantly impact gait kinetics (*Eliashar et al., 2002*; *Roepstorff, Johnston & Drevemo, 1999*).

Among commercially available horseshoes, heart-bar, egg-bar, and open-heel tend to be highly represented (*Aoun, Takawira & Lopez, 2024*). Heart-bar, egg-bar and wooden clog shoes are specifically shaped to shift the ground reaction forces in the palmar/plantar direction, and they facilitate breakover (*Hüppler et al., 2016*; *Rogers & Back, 2003*; *Rogers & Back, 2007*). The continuous shape of both heart-bar and egg-bar shoes increases their surface area compared to a standard shoe, though the heart-bar shoe has greater hoof surface contact due to an extension over the frog. Both shoes are used for a number of functional and therapeutic purposes including alleviating heel pain and support of laminitic hooves (*O'Grady & Parks, 2008*; *Rogers & Back, 2003*). The wooden clog shoe is designed specifically for hooves affected by laminitis. It consists of a 1.9 cm-thick hoof-shaped, wooden platform with a perimeter beveled at an angle of 45° from proximal to distal, and the flat ground surface is covered with flexible rubber material for traction (*O'Grady & Steward, 2009*). A craniocaudal rocking motion from impact through lift off is intended to diminish the torque on the dorsal hoof lamellae by reducing the moment of the deep digital flexor tendon around the distal interphalangeal joint and alleviating breakover stresses (*O'Grady, Steward & Parks, 2007*; *Steward, 2003*).

Based on current knowledge, shoe composition and shape both influence equine gait kinetics, and quantification of their impact on individual ground reaction forces (GRF) provides a comprehensive assessment of the effects (*Eliashar et al., 2002*; *Hagen et al., 2017*; *Pardoe et al., 2001*; *Roepstorff, Johnston & Drevemo, 1999*). The force platform is a validated tool for quantification of GRFs in non-lame and lame horses (*Barrey, 1999*; *Ishihara et al., 2009*). Established measures include vertical ($_V$), braking ($_B$), and propulsion ($_P$) peak

force (PF_V, PF_B, PF_P) and impulse (IMP_V, IMP_B, IMP_P). The contact time with the ground surface during the step cycle is the total stance time (ST), which can be divided into an initial braking followed by a propulsion phase. The resultant GRF force vector in the Y (craniocaudal)-Z (vertical) plane, the vector sum of horizontal and vertical vectors, represents the primary direction and magnitude of the forces between the hoof and ground surface in the sagittal plane (*Clayton & Hobbs, 2019*). The dynamic ratio of GRF_Y/GRF_Z as a representation of the coefficient of friction is often measured during the sliding phase of the stance cycle (*Pardoe et al., 2001*). These kinetic measures make it possible to quantify shoe effects on GRF, temporal step cycle components, and resultant GRF_{YZ} vector angles that, together, compose a complete kinetic gait evaluation.

In addition to shoeing condition, the gait parameters described above are influenced by gait velocity and ground surface characteristics. An increase in speed results in higher $PF_{V,}$ lower IMP, and shorter ST in fore- and hind limbs, and forelimb vertical force curves can have a double-peak at high speeds (*Biknevicius, Mullineaux & Clayton, 2004*; *Dutto et al., 2004*; *Khumsap et al., 2002*; *McLaughlin et al., 1996*; *Weishaupt et al., 2010*). The loading rates, vertical and horizontal components of PF, pressure distribution, and phalangeal alignment are also significantly affected by the type and roughness of the ground surface at a trot or a walk (*Gustås, Johnston & Drevemo, 2006*; *Hüppler et al., 2016*; *Setterbo et al., 2009*).

As mentioned above, shoe configuration impacts gait kinetics. Shoeing alone is reported to increase breakover duration (*Hagen et al., 2021*). A recent kinetic investigation confirmed that the size and shape of caulks to improve traction of iron open-heel shoes differently affect fore- and hind limb equine trotting gait kinetics (*Wang et al., 2021*). Among assessed measures, forelimb PF_V increased the most from unshod with composite plastic-steel shoes, and hind limb PF_B increased the most from unshod with composite plastic-steel shoes followed by open-heel shoes with a thin layer of tungsten carbide, then open heel shoes with low profile-high surface area calks (*Wang et al., 2021*). Differences in pressure distribution on the hoof among shoe shapes have been confirmed in separate investigations (*Hagen et al., 2017*; *Hagen et al., 2016*; *Hüppler et al., 2016*); in one study, pressure peaks occurred at the heels with bar shoes, beneath the ends of the shoe branches at the toe with open toe shoes, and beneath the toe and thin branches of a wide toe shoe in walking horses (*Hüppler et al., 2016*). A recent *in situ* study confirmed distinct hoof capsule deformation behavior among open heel egg-bar, and heart-bar shoes in unaffected and laminitic hooves at cyclic loads up to 5.5×10^3 N (*Aoun et al., 2023*). The novel shape and function of the wooden clog shoe is expected to have distinctive effects on gait kinetics.

To date, quantifiable information about the immediate effects of shoe design on the external forces experienced by the hoof during the stance phase of a walk is limited. Therefore, the primary objective of this *in vivo* study was to quantify equine forelimb walking kinetics while unshod and with open-heel, egg-bar, heart-bar, or wooden clog shoes. Based on distinct hoof deformation characteristics among shoe configurations during dynamic vertical loading *in vitro* and unique pressure distribution among shoe shapes *in vivo*, it was anticipated that equine forelimb kinetic measures at a walk would differ among shoes and while unshod due to dissimilar force distribution on the hoof

surface throughout the step cycle (*Aoun et al., 2023*; *Aoun, Takawira & Lopez, 2024*; *Hagen et al., 2017*; *Hagen et al., 2016*; *Hüppler et al., 2016*). The first tested hypothesis was that vertical, braking, and propulsion PF and IMP are different while shod with heart-bar, egg-bar, open-heel, and wooden clog shoes, or while unshod. The second hypothesis was based on information that shoeing increases breakover duration, egg-bar, heart-bar, and wooden clog shoes facilitate breakover relative to open heel and unshod, and the hoof contact surface area among the three is least with egg-bar and greatest with wooden clog shoes (*Hagen et al., 2021*; *Rogers & Back, 2007*). It was hypothesized that the resultant $\mathbf{GRF_{YZ}}$ vector has the longest duration of cranial angulation with open-heel shoes followed by unshod, then egg-bar and heart-bar shoes, and the shortest with wooden clog shoes. The results of this investigation include unique information about the effect of common shoe configurations on walking gait kinetics of non-lame horses to expand the science of horseshoes, and they include quantifiable data on the potential protective capacity of wooden clog shoes for damaged or weak hooves.

MATERIALS AND METHODS

Ethics and regulations

The study was approved based on the ethical and welfare regulations of the Louisiana State University Institutional Animal Care and Use Committee (IACUCAM-21-157).

Animals and housing

Six horses were selected from the university research herd based on the following inclusion criteria: (1) gelding ($n = 4$) or mare ($n = 2$); (2) light breed; (3) 5 to 25 years (15.3 ± 1.5 years, mean ± standard error of the mean (SEM)); (4) 400 to 600 kg (545.6 ± 69.4 kg); and (5) no subjective lameness. A licensed veterinarian performed physical and lameness examinations to rule out illness, trauma, or lameness prior to study enrollment. The lameness evaluation was performed according to the criteria of the American Association of Equine Practitioners lameness scale. Horses were housed in individual stalls (3.6 × 3.6 m) with wood shaving bedding for at least two days prior to and for the duration of the gait trials (5 days/horse). They had free access to water in a bucket (16 L), about 2.7 kg of commercial feed (Strategy, Purina Animal Nutrition LLC, Shoreview, MN, USA), and four kg of Bermuda grass hay, which were all replenished twice daily.

Shoeing

The hooves of the horses were trimmed on a regular schedule, every 6–8 weeks, by a certified farrier as part of standard husbandry protocol for the university herd. All four hooves of horses included in the study were trimmed by a certified farrier about 12 days before the initial force platform evaluation that was performed while horses were unshod. For purposes of this study, shoes were only applied to forehooves. Commercially available open-heel (Fig. 1A, 300.5–350.1 g, Kerckhaert, Vogelwaarde, The Netherlands), egg-bar (Fig. 1B, 342.5–410.9 g, Ironworks, Texas Farrier Supply, Weatherford, TX, USA), heart-bar (Fig. 1C, 342.9–456.9 g, Ironworks, Texas Farrier Supply, Weatherford, TX,

USA), and wooden clog (Figs. 1D–1F, 144–181.7 g, Equicast, Inc., Lawrence, KS, USA) shoes were used in the study. As indicated above, the shoe weight varied slightly with size and configuration. Shoes were applied in a random order based on a computer-based random number generator (Microsoft Excel, Microsoft, Redmond, WA, USA). Metal shoes were fastened with two nails per side and nail holes were reused between shoes to avoid multiple holes in the hoof wall. The nails were clinched after placement to seat them in the shoe and bend the surface end toward the hoof. For fixation of the wooden clog shoe, sizes were first determined by the farrier based on the hoof width and length. The frog sulci were packed with a two-part silicon-based impression material (Fig. 1D). Then, with the horse standing on the shoe, two wood screws, preplaced at the medial and lateral quarters, were tightened to hold the shoe in place (EDSS, Equine Digit Support System, Inc., Penrose, CO, USA). Subsequently, aliquots (∼5 ml) of fast setting urethane adhesive (HOOFTITE™, Chem Select, Inc., Rancho Santa Margarita, CA, USA) were placed about two cm apart and one cm from the hoof solar margin around the circumference of the hoof (Fig. 1E). Next, moistened 3″ fiberglass casting material (EquiCast®, Equicast, Inc., Lawrence, KS, USA) was wrapped about the outer circumference of the shoe and hoof, and linear low-density polyethylene was applied on top of the cast to facilitate the curing process (Fig. 1F). It was removed after about 5 min.

Kinetic data collection

Horses were walked by experienced handlers over a 900 × 900 mm force platform (Model BP900900, Advanced Mechanical Technology, Inc., Watertown, MA, USA). The force platform was embedded in a ∼40-meter-long concrete runway for GRF data collection. It had a magnetic cover with a thin layer of concrete on the top surface that was the same color and texture as the runway. Light emitting diode markers (LED, 2 × 1 cm) of an active motion detection system (Codamotion®, Charnwood Dynamics, Ltd., Rothley, UK) were attached to the hoof wall using commercially available hook and loop fasteners (1 × 1 cm, Velcro®, Velcro USA, Inc., Manchester, NH, USA) adhered to the markers and hoof surfaces with cyanoacrylate glue. They were attached at the coronary band, the midpoint, and solar margin of the toe and at the coronary band and solar margin of the lateral and medial quarters and heels (Fig. 2, ODIN V2.0, Codamotion®, Codamotion Ltd). An additional marker was attached to a neoprene support boot (Dura-Tech®, Schneiders, Chagrin Falls, OH, USA) at the lateral surface of the fetlock. Two optoelectronic sensor units (Codamotion®) were placed facing each other and the force platform ∼3 m from the center on the x axis. A fixed origin of a virtual cartesian system coordinate axis was established at the center of the force platform. Data from a total of 240 individual trials was recorded at a sampling frequency of 200 Hz with a commercially available software program (ODIN V2.0, Codamotion®, Codamotion Ltd, Rothley, UK), and data was reduced with custom code (Python, The Python Software Foundation, Beaverton, OR, USA). A trial was considered successful if the forelimb hoof fully contacted the platform followed by the ipsilateral hind limb hoof at a speed between 1 to 2.3 m s^{-1}, a range that included a comfortable walking rate for all horses in the study. The acceptable individual variance in individual horse walking speed among all shoe condition trials was a maximum

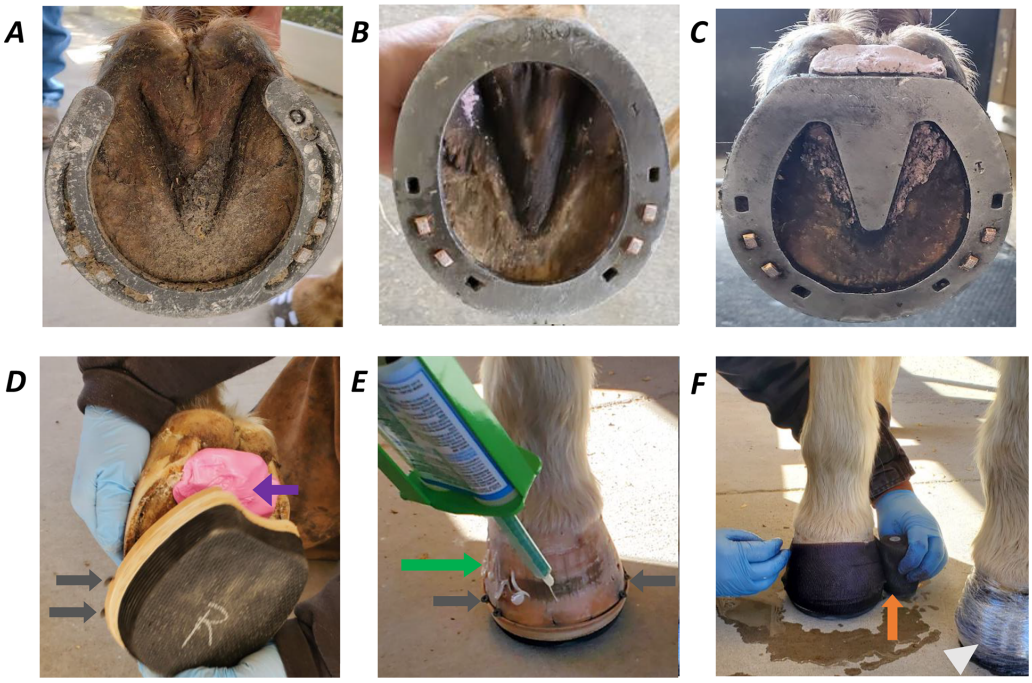

Figure 1 Commercially available shoes used in the study. Force platform data were collected while horses were unshod and then after (A) open-heel, (B) egg-bar, (C) heart-bar, or (D) wooden clog shoes were applied to the forelimbs by a certified farrier in random order. Horses were shod with each shoe type 22–24 h prior to kinetic gait collection. Iron shoes were affixed with two nails per side using the same nail holes for all shoes. A two-part, silicon-based impression material was used to fill the frog sulci (D; purple arrow) prior to application of wooden shoes which were stabilized by compressing hoof tissue under the heads of two screws on each side when the screws were advanced into the wood base (D and E; gray arrows) on each side of the wall. Fast setting resin (E; green arrow) was applied to the hoof wall before fiberglass cast material was added to enclose the dorsal hoof wall and periphery of the wood shoe (F; orange arrow). Linear low-density polyethylene was applied to facilitate curing of the casting material (F; white arrowhead).

Full-size DOI: 10.7717/peerj.18940/fig-1

of ±5%. Trials were rejected if both forelimb and hind limb hooves did not contact the platform, if either hoof was not entirely on the force platform, or if either was within five cm of the perimeter. For each shoeing condition, a total of four successful trials per side (left and right, 8 total) were recorded. Speed was calculated for each trial as the distance between the position of the proximal lateral quarter marker at full stance (resultant GRF_{YZ} vector at 90°) for two consecutive steps (a full stride cycle) divided by the elapsed time between the timestamps for each position as the horse walked across the force platform.

Kinetic data reduction

Forces

Vertical, braking, and propulsion PF (PF_V, PF_B, PF_P) were the maximum value of each force curve normalized to individual animal weight (N kg^{-1}). The PF_V was the highest peak in the vertical force curve, which was the second peak in this study. The area under the force *versus* time curve for the duration of the stance, IMP, was also normalized to weight (N s kg^{-1}). Impulse was calculated as: $IMP_X = \int_0^{100\%} F_X.dt$; with X representing the

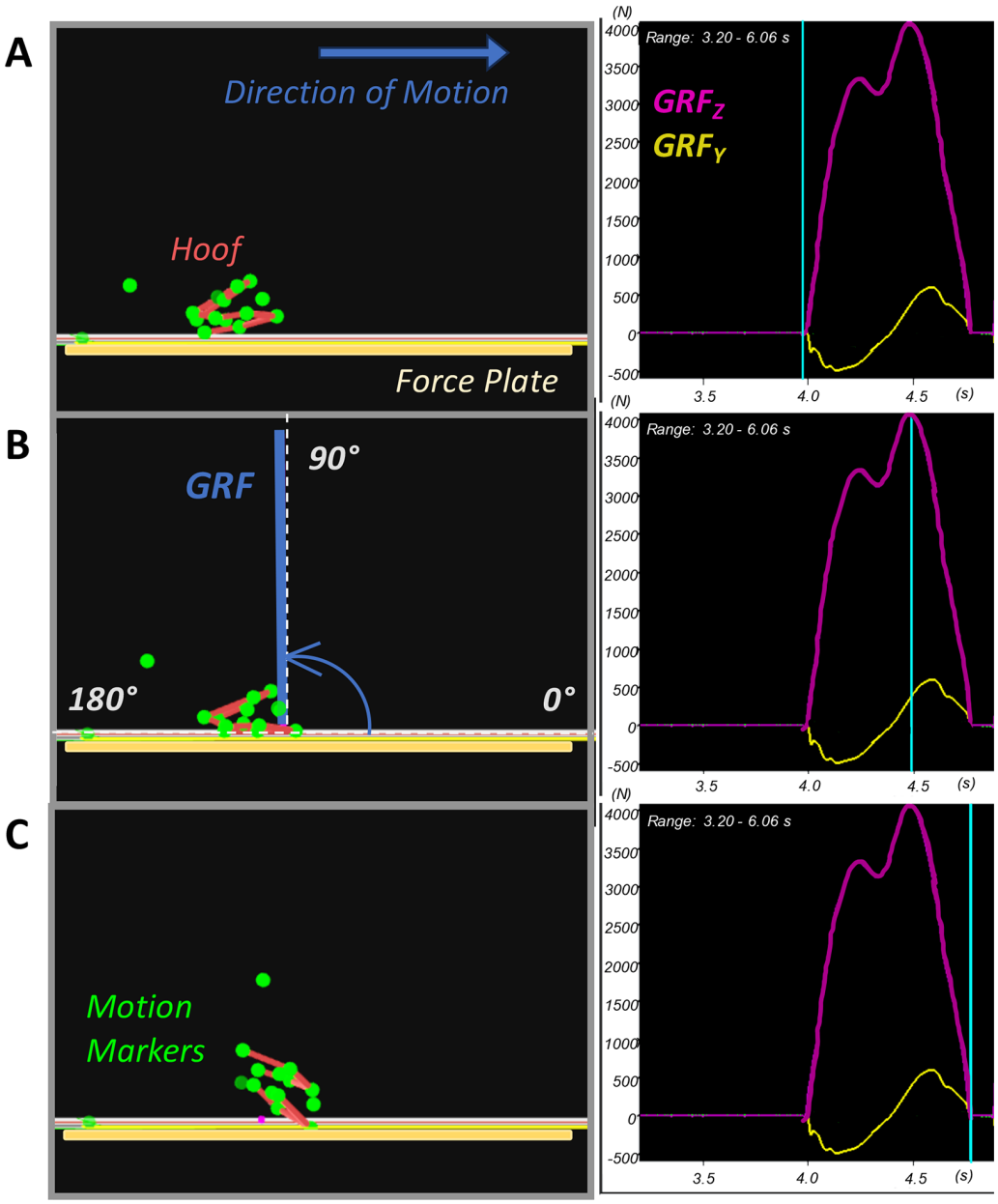

Figure 2 Y–Z resultant force vector data collection. The resultant force vector in the Y (craniocaudal)-Z (vertical) plane, $\mathbf{GRF_{YZ}}$, magnitude and direction were quantified at 5% increments of the step cycle during each gait trial from heel down (A), through full stance (B), to toe off (C).

Full-size DOI: 10.7717/peerj.18940/fig-2

force direction, vertical, caudal (braking), or cranial (propulsion) (IMP_V, IMP_B, IMP_P), respectively.

Peak braking to vertical force ratio

As a representation of traction, the braking to vertical PF ratio was calculated as $\frac{PF_B}{PF_V}$; where PF_B is the peak braking force and PF_V is the peak vertical force (*Burwell & Rabinowicz, 1953*; *Wang et al., 2021*).

Fore- to hind limb vertical peak force ratio

The ratio of the sum of PF_V between fore- and hind limbs for each shoeing condition was determined using PF_V values from combined trials for individual horses. It was calculated as $\frac{SUM(PF_{V\ forelimbs})}{SUM(PF_{V\ forelimbs}+PF_{V\ hind\ limbs})} * 100$ or $\frac{SUM(PF_{V\ hind\ limbs})}{SUM(PF_{V\ forelimbs}+PF_{V\ hind\ limbs})} * 100$ (*Wang et al., 2021*).

Y-Z resultant force vectors

The mean GRF_Y and GRF_Z of all trials for each shoeing condition were used to calculate the resultant ground reaction force vector (GRF_{YZ}) in the Y (craniocaudal)-Z (vertical) plane depicting the magnitude ($|GRF_{YZ}|$) and direction at 5% increments of the step cycle from heel impact through full support (PF_V) to toe off (Fig. 2, ODIN V2.0, Codamotion®, Codamotion Ltd). Vector magnitude and direction were quantified as previously described, except the precise tail of the vectors (center of pressure on the force platform) was not determined in this report (*Hobbs, Robinson & Clayton, 2018*; *Kambhampati, 2007*). The magnitude of the resultant GRF_{YZ} vector in 2D was calculated using the formula: $|GRF_{YZ}| = \sqrt{GRF_Y^2 + GRF_Z^2}$ where GRF_Y and GRF_Z are the vector components in the craniocaudal and vertical directions, respectively. The direction of the GRF_{YZ} vector relative to the horizontal axis at each increment was determined with the Y–Z coordinates of the vector as $\cos^{-1}\left(\frac{GRF_Y}{GRF_Z}\right)$. A vector angle of $0° \leq GRF_{YZ}$ angle $< 90°$ represents a cranial force direction (positive GRF_Y), GRF_{YZ} angle $= 90°$ represents a vertical vector (null GRF_Y), and $90° < GRF_{YZ}$ angle $\leq 180°$ represents a caudal force direction (negative GRF_Y). Graphic representations of the data were generated with commercially available software (Microsoft Excel, Microsoft, Redmond, WA, USA).

Temporal parameters

The ST in seconds (s) was the time between initial contact of the hoof with the force platform to lift off based on a minimum threshold of $PF_V = 50$ N. Time to braking, vertical, and propulsion PF (time to PF_B, time to PF_V, time to PF_P) were the times from initial hoof contact to the maximum value (peak) of each force component. Braking time was the time from initial hoof contact to the point where braking transitioned to propulsion ($GRF_Y = 0$); propulsion time was from the transition point until hoof-lift off. The time to each PF and braking and propulsion times were each determined as a percent of the ST.

Statistical analysis

Data is presented as mean ± standard error of the mean (SEM). All statistical analyses were performed with JMP Pro version 17.0.0 (JMP Statistical Discovery LLC, Cary, NC, 2022–2023). Outcome measures compared among shoeing conditions included PF_V, PF_B,

PF_P, IMP_V, IMP_B, IMP_P, PF_B/PF_V, ratio of the sum of PF_V between fore- and hind limbs, ST, percent time to PF_B, PF_V, and PF_P, and percent braking and propulsion times. Differences among shoes were evaluated using mixed-effects models with horse identification and trial number as random effects and shoeing condition, speed, and their interaction as fixed effects. Interaction between shoeing and speed was evaluated with all mixed models, and none were significantly affected, so the interaction was removed as a covariate. Including speed as a covariate, without its interaction with shoeing, improved the prediction fit for all kinetic variables by a smaller Akaike information criterion (AIC). So, speed was included as a fixed effect in the mixed-effects models used to evaluate differences among shoeing conditions. When the shoeing condition effect was significant, *post hoc* Tukey's tests were employed for multiple comparisons across shoeing conditions. Speed among shoeing conditions was evaluated *via* one-way ANOVA. The normality of the residuals from the parametric models was examined and confirmed by quantile plots. Differences in resultant ground reaction force vector (GRF_{YZ}) magnitude among shoeing conditions were compared at each stance increment with a two-way ANOVA with *post hoc* Tukey's tests when the shoe effect was significant for a given increment. A random forest (RF) classifier algorithm was used to predict shoeing condition from kinetic outcome measures. Shoeing condition was the target variable with all kinetic measures as predictive features. Significance was consistently set at p-value < 0.05.

RESULTS

Gait speed

The speed for trials included in the data analysis was 1.51 ± 0.02 m s^{-1}. Specific to shoeing condition, the speed was 1.55 ± 0.03 m s^{-1}, 1.55 ± 0.04 m s^{-1}, 1.42 ± 0.03 m s^{-1}, 1.51 ± 0.04 m s^{-1}, and 1.51 ± 0.03 m s^{-1} for egg-bar, heart-bar, open-heel, and wooden clog shoes, and while unshod, respectively (Fig. S1). Speed was not significantly different among shoeing conditions.

Ground reaction force components and impulses

The PF_V was significantly affected by shoeing condition (p-value $= 0.0002$, Fig. 3); it was highest with egg-bar (6.35 N kg$^{-1} \pm 0.1$) shoes followed, in order, by unshod (6.32 N kg$^{-1} \pm 0.1$), and then with heart-bar (6.27 N kg$^{-1} \pm 0.1$), open-heel (6.23 N kg$^{-1} \pm 0.1$), and wooden clog (6.13 N kg$^{-1} \pm 0.1$) shoes. The PF_V with wooden clog shoes was lower than with egg-bar shoes (p-value $= 0.0002$) or when unshod (p-value $= 0.002$). Similarly, the PF_P was significantly affected by shoeing condition (p-value < 0.0001, Fig. 3). The PF_P was higher with wooden clog (0.81 N kg$^{-1} \pm 0.03$) *versus* open-heel (0.71 N kg$^{-1} \pm 0.03$, p-value < 0.0001) or egg-bar (0.75 N kg$^{-1} \pm 0.03$, p-value $= 0.01$) shoes or while unshod (0.74 N kg$^{-1} \pm 0.03$, p-value $= 0.004$), and lower with open-heel compared to heart-bar shoes (0.77 N kg$^{-1} \pm 0.03$, p-value $= 0.02$). The IMP_V, significantly affected by shoeing condition (p-value $= 0.011$), was lower while unshod (3.16 N s kg$^{-1} \pm 0.09$) compared to with open-heel (3.28 N s kg$^{-1} \pm 0.09$, p-value $= 0.009$) or wooden clog (3.26 N s kg$^{-1} \pm 0.09$, p-value $= 0.04$) shoes. The IMP_B, significantly affected by shoeing condition

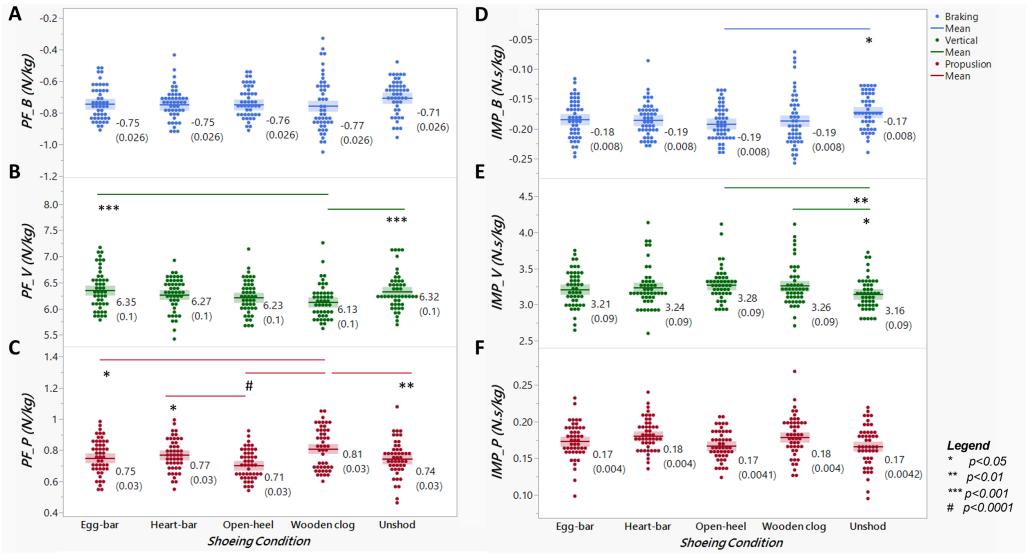

Figure 3 Peak ground reaction forces (PF) and impulses (IMP) across distinct shoeing conditions. Braking (A-PF_B, D-IMP_B), vertical (B-PF_V, E-IMP_V), and propulsion (C-PF_P, F-IMP_P) peak forces (A–C) and impulses (D–F) normalized to body weight from horses ($n = 6$) shod with egg-bar, heart-bar, open-heel, or wooden clog shoes and while unshod. Points in the graph represent individual trials, and the horizontal line in the middle of each set indicates the mean; the numeric mean value along with the standard error of the mean (in parentheses) are shown to the right of each data set. Significant differences between data sets with a line between them are indicated by a symbol beneath the line.

Full-size DOI: 10.7717/peerj.18940/fig-3

(p-value = 0.0403), was higher with open-heel (-0.19 N s kg^{-1} $\pm$ 0.008) shoes compared to unshod (-0.17 N s kg^{-1} $\pm$ 0.008, p-value = 0.02).

Peak braking to vertical force ratio and vertical peak force distribution

The ratio of PF_B/PF_V, significantly affected by shoeing condition (p-value = 0.024), was lowest when horses were unshod (0.11 $\pm$ 0.004), though only significantly lower compared to when shod with wooden clog (0.12 $\pm$ 0.004, p-value = 0.015, Fig. 4) shoes. The forelimb:hind limb ratio of the sum of total PF_V was about 60%:40% for all shoeing conditions, and it was not significantly different among them (Fig. 5).

Temporal parameters

Shoeing condition significantly affected the percent times to PF_V, PF_B and PF_P (p-value < 0.0001); all three were greater with wooden clog shoes *versus* other shoes and when unshod (Fig. 6). Percent time to $PF_P$was also greater with open-heel (75.22 $\pm$ 1.1%) *versus* egg-bar shoes (73.65 $\pm$ 1.1%, p-value = 0.03). The percent of stance time for braking was greater and that for propulsion was lower in horses with wooden clog shoes than with all other shoes or when unshod (Fig. 7; p-value < 0.0001).

Though not significantly different among shoeing conditions, the ST was shortest when unshod and longest with open-heel shoes (Fig. 8). The data point distribution was distinct among shoeing conditions. Most of the individual ST data points with open-heel and

Figure 4 Braking to vertical peak force ratio among shoeing conditions. The PF_B/PF_V ratio from horses ($n = 6$) shod with egg-bar, heart-bar, open-heel, or wooden clog shoes and while unshod. Points in the graph represent individual trials, and the horizontal line in the middle of each set indicates the mean; the numeric mean value along with the standard error of the mean (in parentheses) are shown to the right of each data set. Significant differences between data sets with a line between them are indicated by a symbol beneath the line.

Full-size DOI: 10.7717/peerj.18940/fig-4

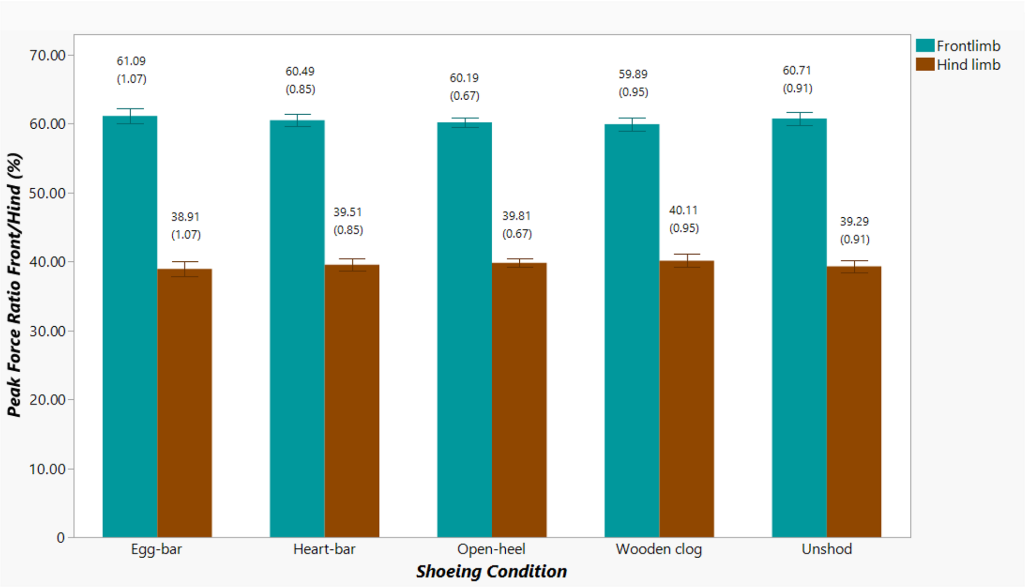

Figure 5 Forelimb (cyan) and hind limb (brown) ratio of the sum of total PF_V among shoeing conditions. Percent forelimb and hind limb vertical peak force distribution from horses ($n = 6$) shod with egg-bar, heart-bar, open-heel, or wooden clog shoes and when unshod. Mean and standard error of the mean (in parentheses) values are shown above each column.

Full-size DOI: 10.7717/peerj.18940/fig-5

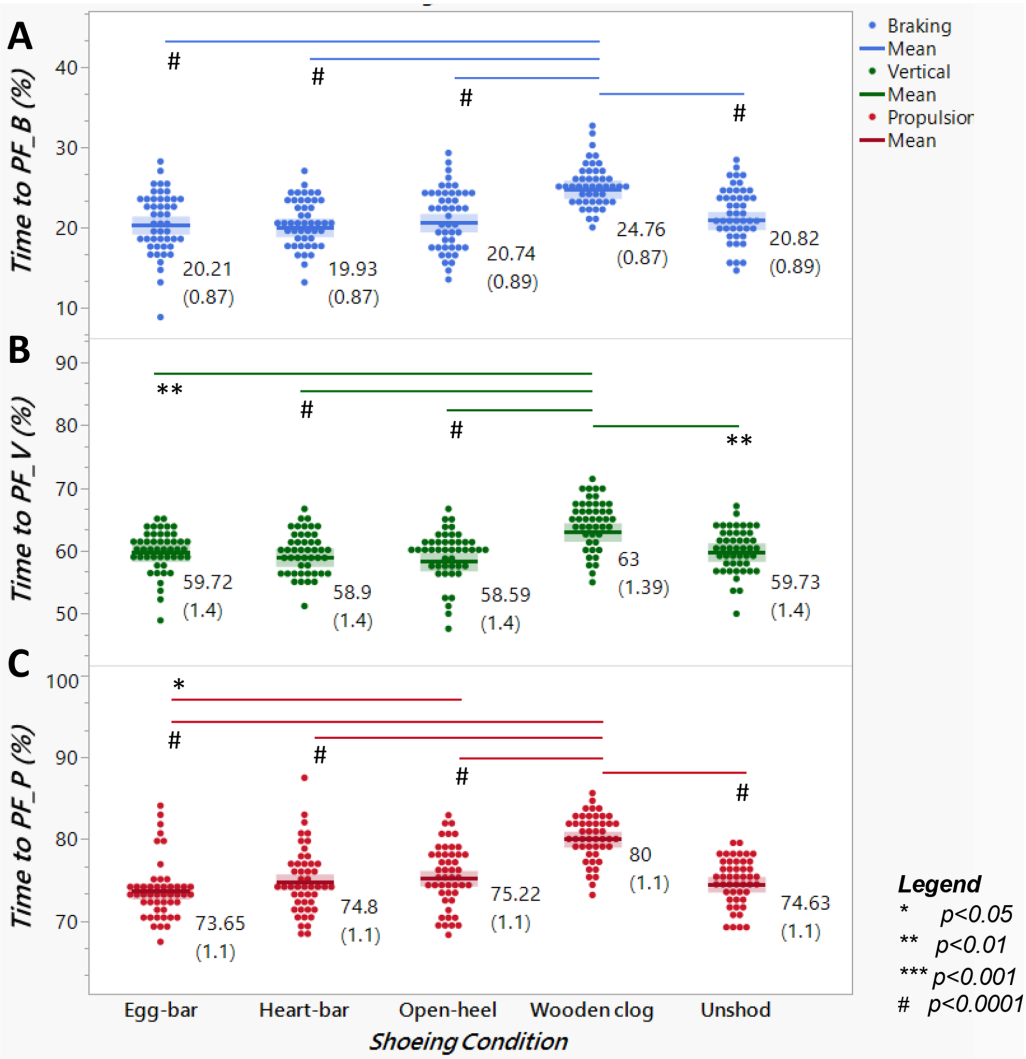

Figure 6 Time to peak force as a percent of stance time among distinct shoeing conditions. Time to (A) braking (PF_B), (B) vertical (PF_V), or (C) propulsion (PF_P) peak force from horses ($n = 6$) shod with egg-bar, heart-bar, open- heel, or wooden clog shoes and while unshod. Points in the graph represent individual trials, and the horizontal line in the middle of each set indicates the mean; the numeric value along with the standard error of the mean (in parentheses) are shown to the right of each data set. Significant differences between data sets with a line between them are indicated by a symbol beneath the line.

Full-size DOI: 10.7717/peerj.18940/fig-6

wooden clog shoes or while unshod were condensed around the medians, while those with egg-bar and heart-bar shoes were widely distributed above and below the median (*i.e.*, higher interquartile range).

Y-Z resultant force vectors

The resultant force vectors, GRF_{YZ}, were initially directed caudally and transitioned to a cranial direction at about midway through the step cycle for all shoeing conditions, though the point of transition from braking to propulsion occurred a bit later in the step cycle (~55%) with the wooden clog shoe compared to other shoeing conditions (~52%) (Fig. 9).

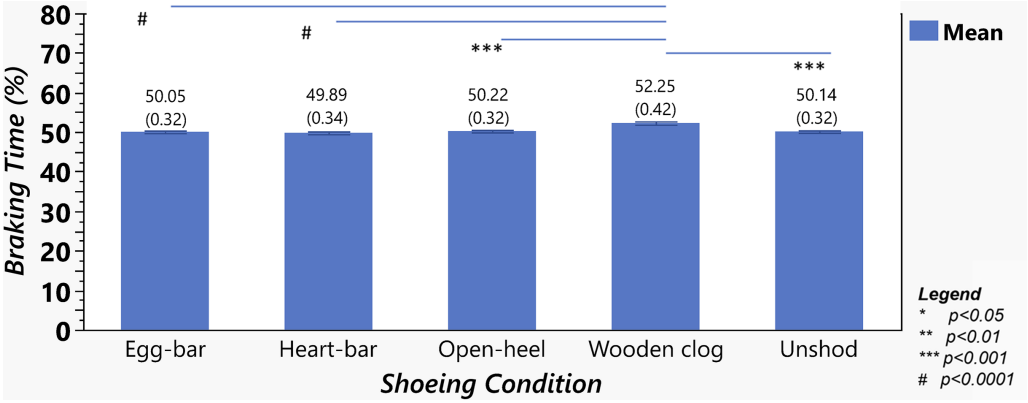

Figure 7 Braking time as a percent of total stance time among shoeing conditions. Percent (mean ± SEM) of stance time in braking from horses ($n = 6$) shod with egg-bar, heart-bar, open-heel, or wooden clog shoes and while unshod. Significant differences between data sets with a line between them are indicated by a symbol beneath the line. Mean and standard error of the mean (in parentheses) values are shown above each column.

Full-size DOI: 10.7717/peerj.18940/fig-7

The vector magnitude had two peaks for all shoeing conditions, one at about 35% of the step cycle and another at 65% of the step cycle for the wooden clog shoe and at 60% of the step cycle for the rest. The magnitudes of the resultant vectors with the wooden clog shoe were less than the other shoeing conditions during the loading phase, greater at the first peak, less at the second peak, and greater during unloading. Also unique to the wooden clog shoe was a decrease in magnitude between the two peaks in contrast to the other shoes for which the magnitude plateaued slightly around the first peak but continued to increase throughout the distance between peaks. While unshod, the magnitude of GRF_{YZ} was lower than the other shoeing conditions during the first peak. Significant differences included that the GRF_{YZ} was less with the wooden clog *versus* egg-bar and hear-bar shoes at 5% of the step cycle and less than all other shoeing conditions at 10% and 15% of the step cycle (Table 1). It was greater with the wooden clog shoe compared to unshod at 30% and 35% of the step cycle. The magnitude was less with the wooden clog *versus* open-heel shoe at 50% of the step cycle, less with the wooden clog shoe *versus* all other shoeing conditions at 55%, and less than with egg-bar shoes and while unshod at 60%. It was greater with the wooden clog shoe than while unshod or with heart-bar or open-heel shoes at 70% of the step-cycle, and greater than all other shoeing conditions at 75–90% of the step cycle.

Shoeing condition classification with a random forest model

The PF_B was highly correlated with IMP_B (0.9, p-value < 0.001) as well as the PF_B/PF_V ratio (0.94, p-value < 0.001) (Fig. S2). The IMP_B was highly correlated with the PF_B/PF_V ratio (0.89, p-value < 0.001). Similarly, PF_P was highly correlated with IMP_P (0.75, p-value < 0.001) and moderately correlated with percent ST to PF_V (0.62, p-value < 0.001). The percent of ST to PF_B and to PF_P were moderately correlated (0.47, p-value < 0.001). The observed correlations were expected due to interdependence among variables.

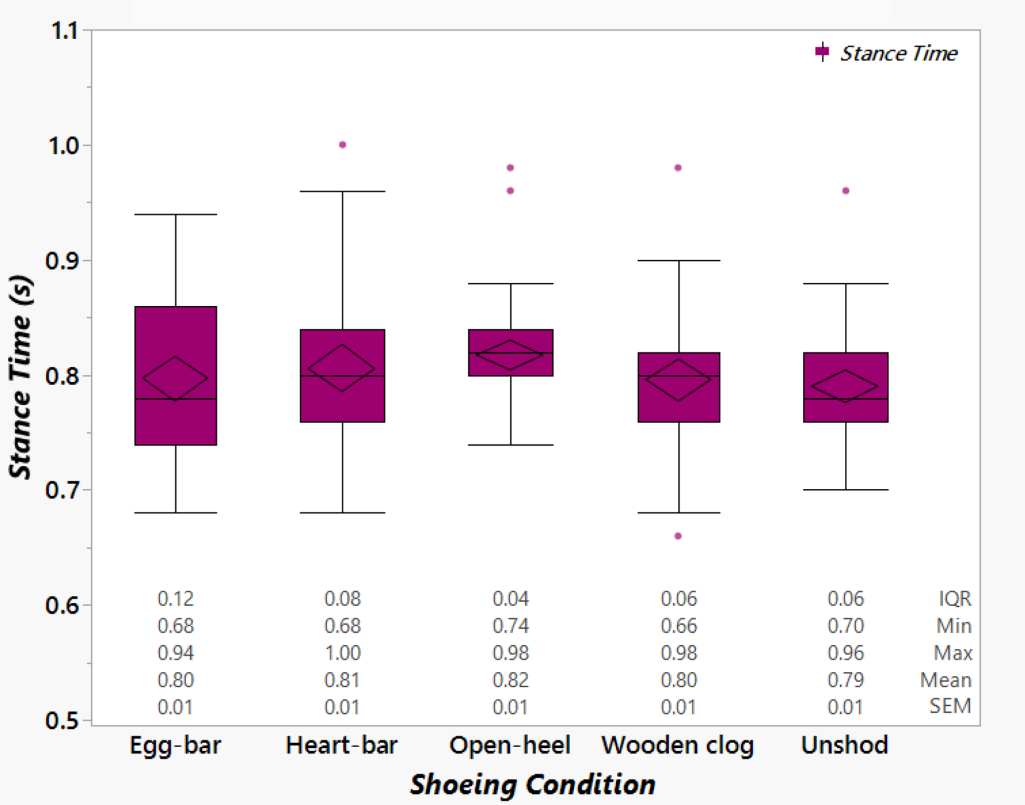

Figure 8 Stance time among shoeing conditions. Box plots showing the stance time from horses ($n = 6$) shod with egg-bar, heart-bar, open-heel, or wooden clog shoes and while unshod. The values below each data set are the interquartile range (IQR), minimum value (Min), maximum value (Max), mean (Mean) and standard error of the mean (SEM).

Full-size DOI: 10.7717/peerj.18940/fig-8

The RF model could predict shoeing condition from kinetic measures with an accuracy of about 41%. The wooden clog shoe (F1-score = 1.0) could be predicted with higher positivity than the unshod and egg-bar shoes (F1-score = 0.38) which could be predicted with a higher positivity than heart-bar and open-heel shoes (F1-score $\leq$ 0.29) (Fig. 10A). The model had an asymptotic training error curve along the x axis at a tree depth higher than 7, and the classification error was between 0.8 and 0.6 up to that depth (Fig. 10B). Shoeing condition classification relied on all features included in the model but most heavily on percent ST to $PF_{P,}$ percent ST to PF_V, and PF_P (Fig. 10C). Taken together, these results indicate that wooden clog shoes were highly and accurately predictable with the RF model using the kinetic measures included in this study as features.

DISCUSSION

Results of this *in vivo* study establish the effects of shoe configuration on equine gait kinetics at a walk. The first hypothesis, vertical, braking, and propulsion PF and IMP are different while shod with heart-bar, egg-bar, open-heel, and wooden clog shoes, or while unshod, was rejected since pairwise comparisons between shoeing conditions confirmed that not all

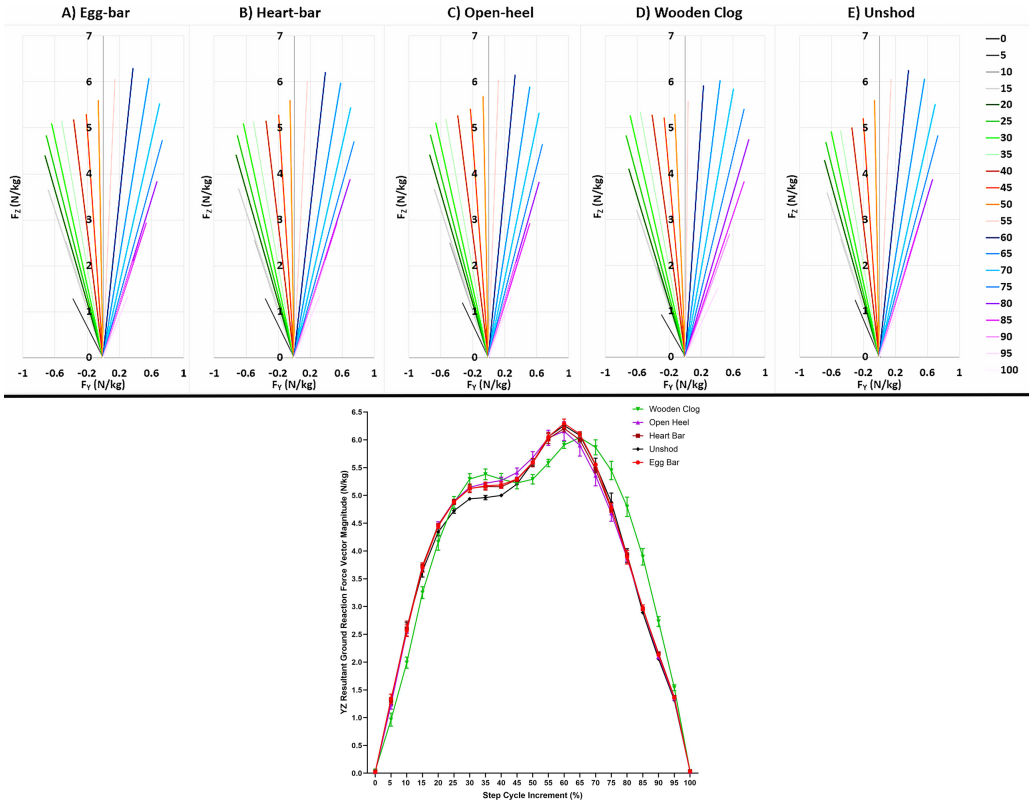

Figure 9 Y–Z resultant ground reaction force vector diagrams and magnitude. Force vectors (upper panel) and vector magnitude (mean ± SEM, lower panel) from forelimbs of horses ($n = 6$) walking over a force platform embedded in a 40-m concrete runway in 5% increments of the complete step cycle while shod with egg-bar (A, red), heart-bar (B, brown), open-heel (C, lavender), or wooden clog shoes (D, green) or while unshod (E, black). In the upper panel each line is the mean value of all horses for the indicated increment and shoeing condition. Specific ranges of the step cycle are shown in shades of grey (0–15%), green (20–35%), orange (40–55%), blue (60–75%), and purple (80–100%), respectively.
Full-size DOI: 10.7717/peerj.18940/fig-9

measures were significantly unique. The second hypothesis, the resultant GRF_{YZ} vector has the longest duration of cranial angulation with open-heel shoes followed by unshod, then egg-bar and heart-bar shoes, and the shortest with wooden clog shoes, was rejected because it was not supported by the GRF_{YZ} vector angle distribution. In fact the cranial angulation was slightly longer with the wooden clog shoes. Although the hypotheses were rejected, the kinetic values compose a unique set of measures for each shoe configuration. Several force measures and most temporal parameters with wooden clog shoes were different from unshod and with the other shoes. Resultant GRF_{YZ} vectors had a slightly broader distribution over the step cycle and a later transition from braking to propulsion with wooden clog shoes relative to other shoeing conditions. Variations in vector magnitude at distinct points during the step-cycle confirmed unique patterns among shoeing conditions with the highest number of significant differences between the wooden clog shoe and the others. Kinetic measures (features) had distinct, clear correlations with the target variable (shoeing condition) when horses were shod with wooden clog shoes compared to other

Table 1 Fyz vector magnitude (mean ± SEM) for 5% step cycle increments.

GRFyz (N/kg)	Egg bar		Heart bar		Open heel		Wooden clog		Unshod	
Step cycle increment	Mean	SEM	Mean	SEM	Mean	SEM	Mean	SEM	Mean	SEM
0	0.02	0.00	0.03	0.02	0.02	0.01	0.05	0.01	0.02	0.00
5	1.34[a]	0.09	1.32[a]	0.04	1.24[ab]	0.09	0.96[b]	0.12	1.28[ab]	0.05
10	2.57[a]	0.11	2.60[a]	0.14	2.55[a]	0.08	1.99[b]	0.10	2.62[a]	0.09
15	3.70[a]	0.08	3.74[a]	0.03	3.72[a]	0.04	3.25[b]	0.11	3.64[a]	0.11
20	4.45	0.04	4.47	0.01	4.47	0.06	4.16	0.15	4.34	0.07
25	4.88	0.02	4.88	0.05	4.90	0.03	4.87	0.11	4.72	0.05
30	5.12[ab]	0.06	5.13[ab]	0.08	5.15[ab]	0.02	5.29[a]	0.10	4.94[b]	0.00
35	5.17[ab]	0.07	5.16[ab]	0.06	5.22[ab]	0.03	5.38[a]	0.10	4.96[b]	0.04
40	5.19	0.06	5.16	0.01	5.27	0.06	5.29	0.10	5.00	0.03
45	5.30	0.02	5.28	0.04	5.41	0.08	5.22	0.10	5.20	0.02
50	5.60[ab]	0.03	5.59[ab]	0.07	5.68[a]	0.11	5.29[b]	0.09	5.59[ab]	0.06
55	6.05[a]	0.07	6.02[a]	0.09	6.04[a]	0.14	5.58[b]	0.07	6.06[a]	0.08
60	6.29[a]	0.08	6.21[ab]	0.06	6.16[ab]	0.17	5.91[b]	0.06	6.26[a]	0.04
65	6.10	0.04	6.00	0.01	5.90	0.19	6.04	0.10	6.08	0.04
70	5.56[ab]	0.02	5.47[a]	0.06	5.36[a]	0.19	5.86[b]	0.13	5.55[a]	0.12
75	4.78[a]	0.08	4.75[a]	0.04	4.68[a]	0.14	5.45[b]	0.16	4.88[a]	0.17
80	3.89[a]	0.12	3.94[a]	0.01	3.87[a]	0.05	4.79[b]	0.17	3.91[a]	0.13
85	2.98[a]	0.05	2.96[a]	0.03	2.96[a]	0.02	3.90[b]	0.15	2.89[a]	0.03
90	2.13[a]	0.03	2.16[a]	0.03	2.11[a]	0.05	2.73[b]	0.09	2.06[a]	0.00
95	1.36	0.03	1.37	0.00	1.35	0.03	1.54	0.06	1.32	0.02
100	0.03	0.01	0.03	0.00	0.03	0.00	0.04	0.00	0.03	0.00

Notes.
Values with distinct superscripts within a row are significantly different among shoeing conditions (p-value < 0.05).

shoeing conditions as indicated by the prediction accuracy of the RF classification. Results of this investigation provide a novel perspective about how equine gait kinetics at a walk are altered by application of the shoes in this study. This new information is useful to understand the kinetic impacts of shoe design.

The unique configuration and composition of the wooden clog shoe likely contributed to lower PF_V given that there were no significant differences in stance time and speed to which to attribute the distinction. This could be a result of both the lower stiffness of the wood composition compared to the iron-based shoes and higher contact surface area (*Fajdiga, Šubic & Kovačič, 2021*; *Moyer & Anderson, 1975*). Reports assessing the direct effect of shoe stiffness on impact force and GRF magnitude in humans confirm that both increase with increasing shoe stiffness; the higher GRF magnitude impacts proximal joint moments and range of motion (*Boyer et al., 2012*; *Lin et al., 2017*; *Teoh et al., 2013*). A lower PF_V with wooden clog shoes also likely contributed to the slightly higher PF_B/PF_V ratio, a representation of interactions between the hoof and ground surfaces, compared to unshod. Reducing the ratio indicates decreased grip, which could also be a benefit from less jarring during hoof deceleration (*Parkes & Witte, 2015*). The ratio values in this study are

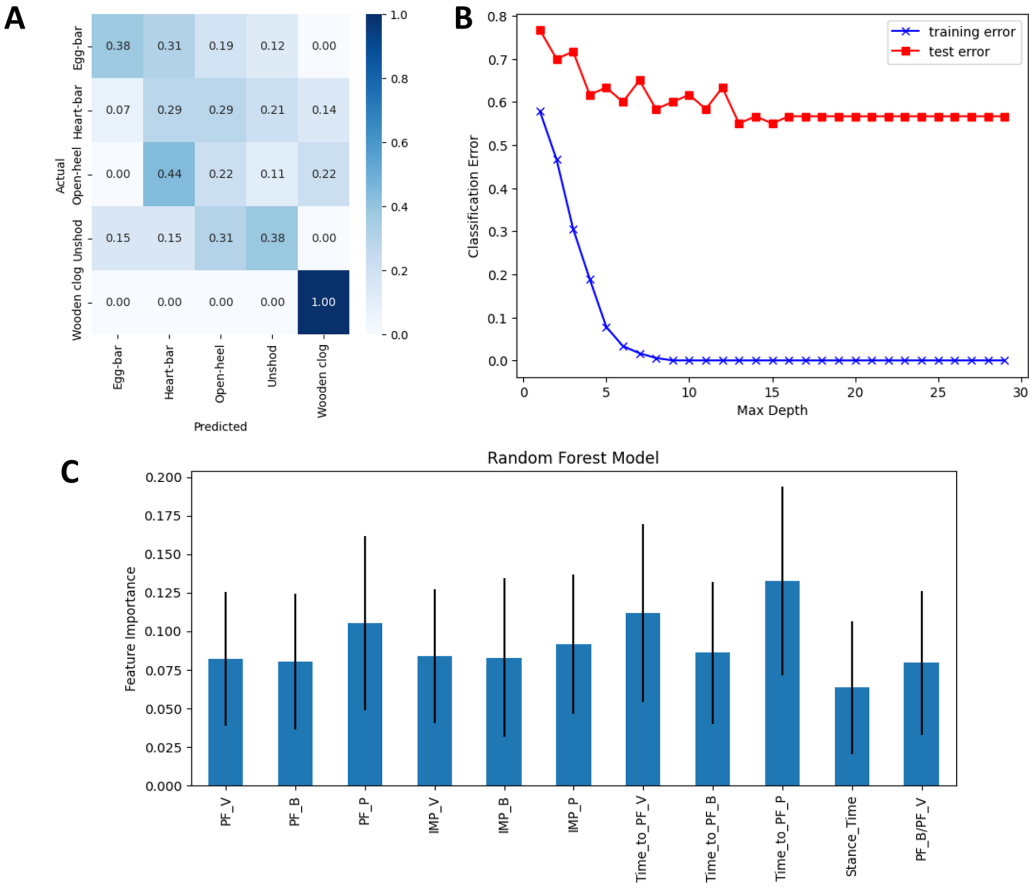

Figure 10 **Random forest model outcomes.** (A) Confusion matrix for the RF model to predict shoeing condition from kinetic variables with each cell across the matrix diagonal showing the percent of true predictions and all other cells showing false predictions. (B) Training (blue) and test (red) error curves against different maximum tree depths in the RF model used to predict shoeing condition. (C) Feature importance (mean ± SEM) of each variable in the random forest algorithm classification model to predict shoeing condition from kinetic variables.

Full-size DOI: 10.7717/peerj.18940/fig-10

aligned with those in a previously published kinetic study, though ground and hoof surface properties contribute to differences among investigations (*Chateau et al., 2010*; *Lewis et al., 2015*; *Pardoe et al., 2001*; *Parkes & Witte, 2015*; *Wang et al., 2021*).

The efficacy of the beveled shape of the wooden clog shoe to facilitate breakover is supported by the highest percent stance in braking and lowest in propulsion in this study (*O'Grady, 2020*). Specifically, the beveled shoe shape is thought to shorten the breakover distance by moving it in a palmar/plantar direction like a rolled toe shoe (*Van Heel, VanWeeren & Back, 2006*). In a previous study, the distal interphalangeal joint moment arm during breakover was reduced by natural balance (rolled toe) and quarter-clip shoes compared to toe-clip shoes, but the peak distal interphalangeal joint moment was not significantly different between shoes (*Eliashar et al., 2002*). Additional research is necessary to investigate if the same is true with wooden clog shoes. The longer times to reach the peak of all forces with wooden clog shoes was also likely a consequence of the unique shape,

which was unfamiliar to the horses in this study and has been shown to decrease the limb loading rate in humans wearing rocker-soled shoes compared to barefoot (*Lin et al., 2017*). Even though total stance time was not different, the rocking motion, and, potentially, the increased shoe height, required additional time to reach the peak force levels in all planes evaluated. Together, the study results confirm that the wooden clog shoe facilitates breakover and reduces peak vertical forces experienced by the limb during the second half of stance, effects that could benefit horses with distal joint pain and/or weakened hooves without greater force distribution to the rear limbs.

In contrast to the kinetic changes observed with the wooden clog, PF and IMP were fairly consistent among iron shoe shapes in this study as previously reported, though the results of this study are specific to forelimbs at a walk and results vary due to different gaits, velocities, and shoes among investigations (*Amitrano, Gutierrez-Nibeyro & Schaeffer, 2016*; *Khumsap et al., 2002*; *Weishaupt et al., 2010*). Changes in braking are especially meaningful given the greater braking function of the equine forelimbs (*Dutto et al., 2004*; *Hobbs & Clayton, 2013*). The higher IMP_B with open-heel shoes *versus* unshod might be explained by the slightly higher PF_B and percent braking time since the measure represents the area under the force *versus* time curve. The mass of the open-heel shoe may also have contributed to differences between the two conditions since a greater mass from the shoe can increase landing velocity of the hoof and result in a greater force at impact during the braking phase of the stance (*Parkes & Witte, 2015*).

The longer stance time with open-heel shoes could have contributed to the higher IMP_V, despite a lower PF_V. Though trial speed was not significantly different among shoeing conditions, it was slightly lower, 0.09 ms^{-1}, with open-heel shoes compared to unshod, and it might have contributed to the higher IMP_V and lower PF_V values with the shoes. Another explanation is that the PF_V point in this study occurred during the second half of the stance phase. The GRF_{YZ} had a lower magnitude during the first peak while unshod compared to with open-heel shoes while the relationship reversed during the higher second peak. As such, and as indicated above, the PF_V and IMP_V values and comparisons reported here are specific to the second half of the stance. These points highlight the complexity of equine gait kinetics at a walk where the vertical forces have two peaks during the step cycle.

Graphs of the mean resultant vectors in the sagittal plane during the stance phase provide a broad perspective of variations in gait kinetics attributable to shoe configuration. The GRF_{YZ} vector direction changes from caudal to cranial angulation at the point of full stance with unshod hooves, corresponding to horizontal decelerative followed by accelerative forces during stance (*Hobbs & Clayton, 2013*). The vector origin is affected by pressure distribution over the hoof surface, and it is impacted by alterations in pressure distribution over the hoof surface with shoes (*Barrey, 1990*; *Parks, 2003*); the vector direction depends on the magnitude of braking and propulsive forces. The results confirm unique shapes of the vector magnitude over the course of the step cycle and support the individual force data. Specifically, the magnitude was greatest with the wooden clog shoe during the first peak, but it was significantly lower during the higher second peak that corresponded to PF_V. The distinct decrease in the magnitude between the two peaks with the wooden

clog shoe is consistent with GRF forces applied across the larger, convex surface area and rocking motion during the transition from braking to propulsion. Additionally, the higher magnitudes with the wooden clog shoe during the propulsion phase are consistent with the higher PF_P as is the lower magnitude during braking while unshod which had the lowest PF_B and IMP_B. A slightly delayed transition to propulsion with the wooden clog shoe coincides with the greater braking ST percentage with the shoe. Despite higher forces during the first half of the stance and higher propulsive forces during the second half, the lower PF_V with the wooden clog shoe could reduce hoof stresses and benefit weakened or damaged tissues. Similarly, the smoother breakover could reduce distal interphalangeal joint extension, reduce deep digital flexor tendon strain, and decrease pressure on the navicular joint during the final part of the stance (*Hagen et al., 2021*). The sagittal plane resultant GRF_{YZ} vector analysis in this investigation expands current understanding of the impact of shoes on kinetic forces experienced by the hoof and forelimb at a walk. Potential long-term implications of the vector distributions for the hoof and distal limb will require additional study.

Use of a RF machine learning algorithm to predict shoeing from kinetic measures determined in this study showed that the wooden clog shoe was classified with the highest accuracy. It is not surprising that the percent ST to PF_V and PF_P and the PF_P had the highest importance for the model since the parameters tended to be among the most distinctive for the wooden clog shoe. The model did not perform well for the other shoeing conditions as they all had poor F-1 scores (less than 0.5). The performance could be related to an insufficient number of data points in the training phase of the model, especially since the measures were relatively similar among shoeing conditions apart from the wooden clog shoe. Similar values within features for different target variables can negatively impact the accuracy of machine learning algorithms, so increasing the number of features and feature data points might improve model accuracy. Highly correlated features can decrease model accuracy; removal of some features might improve model performance. The fact that shoeing conditions could be distinguished from each other using the data from this single study indicates that machine learning algorithms could provide another data analysis mechanism that could substantially expand current knowledge of the relationship between shoe configuration and gait kinetics.

This study was limited by the number of horses included, six light breed horses between 5 and 25 years old. Though the horses were objectively and subjectively not lame, variations in kinetic measures due to subtle limb or hoof pain cannot be entirely ruled out. This could have contributed to intra- or inter-individual differences that reduced statistical power. The study results might also not apply to all horses due to natural variability, including gait variations, among biological subjects. The speed range in this study was relatively wide compared to other studies, though speed did not vary significantly among trials. Hence, the range includes natural variation in a comfortable walking speed among horses included in the study. The results are limited to forelimbs and the shoes included in the study at a walking gait, and peak kinetic values to the second half of the stance. Shoes with similar configurations but with different thickness, mass, or material composition could influence the gait differently (*Pardoe et al., 2001*; *Rogers & Back, 2003*; *Wang et al., 2021*). The study

results also do not take into consideration the breathability of the tested horseshoes, and this property is critical in the design of prosthetics and shoes (*Aflatoony, 2019*; *Pereira et al., 2007*). Effects of shoe material and shape on shear forces, hoof stability, and joint torque, especially given the distinct height and composition of the wooden clog shoe, are important outcomes to be considered for future study designs. A longer period of time with each shoe configuration, typical of a standard shoeing interval, might have allowed for more acclimation and could have resulted in fewer differences among shoes (*Heel, Weeren & Back, 2006*). Additionally, the ground surface for gait trials in this study was concrete. Different ground surfaces will likely have different results (*Crevier-Denoix et al., 2010*; *Robin et al., 2009*).

CONCLUSION

The results of this study provide novel information and unique demonstrations of the impact of shoe shape on equine gait kinetics. The distinctive and highly predictable changes in gait kinetics with the wooden clog shoe were clear, supporting their use to reduce forces experienced by hooves and distal limbs during the second half of stance and during breakover, though higher forces during the first half of stance and during propulsion are important to consider. The altered gait kinetics could potentially protect laminitic hooves and alleviate discomfort from distal interphalangeal joint, distal deep digital flexor tendon, and/or navicular bone pathology. Additionally, machine learning algorithms might eventually improve the ability to design and select shoes intended for hoof protection and function by confirming that they have sufficient impact on target gait kinetics to be identified. Taken together, the results of this study enhance knowledge of shoe effects on equine kinematics at a walk and highlight cutting-edge tools to quantify them.

Abbreviations

PF_V	Peak vertical force (N kg^{-1})
PF_B	Peak braking force (N kg^{-1})
PF_P	Peak propulsion force (N kg^{-1})
IMP_V	Vertical impulse (N s kg^{-1})
IMP_P	Propulsion impulse (N s kg^{-1})
PF_B/PF_V ratio	Ratio of braking to vertical peak forces (–)
ST	Stance Time (s)

ACKNOWLEDGEMENTS

This work was only possible with the help of previous and current LECOR members with data collection. The authors also acknowledge Ms. Cindy Meeker for her professional farrier work, Drs. David Schaeffer and Chin-Chi Liu for assistance with statistical analysis, and Mr. Michael Keowen and Mr. John-Ross Miller for their help with horse husbandry.

ADDITIONAL INFORMATION AND DECLARATIONS

Funding

This work was supported by the Tynewald Foundation, a Charles V. Cusimano Equine Health and Sports Performance Grant, and the Louisiana State University School Department of Veterinary Clinical Sciences. The funders had no role in study design, data collection and analysis, decision to publish, or preparation of the manuscript.

Grant Disclosures

The following grant information was disclosed by the authors:
Tynewald Foundation, a Charles V. Cusimano Equine Health and Sports Performance Grant.
Louisiana State University School Department of Veterinary Clinical Sciences.

Competing Interests

The authors declare there are no competing interests.

Author Contributions

- Rita Aoun conceived and designed the experiments, performed the experiments, analyzed the data, prepared figures and/or tables, authored or reviewed drafts of the article, and approved the final draft.
- Zaneta Ogunmola performed the experiments, analyzed the data, prepared figures and/or tables, and approved the final draft.
- Anaïs Musso performed the experiments, analyzed the data, authored or reviewed drafts of the article, and approved the final draft.
- Takashi Taguchi performed the experiments, analyzed the data, prepared figures and/or tables, and approved the final draft.
- Catherine Takawira performed the experiments, authored or reviewed drafts of the article, and approved the final draft.
- Mandi J. Lopez conceived and designed the experiments, performed the experiments, analyzed the data, prepared figures and/or tables, authored or reviewed drafts of the article, and approved the final draft.

Animal Ethics

The following information was supplied relating to ethical approvals (i.e., approving body and any reference numbers):

The Louisiana State University Institutional Animal Care and Use Committee provided careful review and approval for this research (Protocol: IACUCAM-21-157). Based on Animal Welfare Assurance #A3612-01, License #72-3; Multiple Assurance #M1128.

Data Availability

The following information was supplied regarding data availability:

The raw data are available in the Supplemental Files.

Supplemental Information

Supplemental information for this article can be found online at http://dx.doi.org/10.7717/peerj.18940#supplemental-information.

REFERENCES

Aflatoony L. 2019. Flex, breathe, fit, and walk: exploring technologies accessible in academia for design and production of a custom fit shoes. In: *International textile and apparel association annual conference proceedings*.

Amitrano FN, Gutierrez-Nibeyro SD, Schaeffer DJ. 2016. Effect of hoof boots and toe-extension shoes on the forelimb kinetics of horses during walking. *American Journal of Veterinary Research* **77(5)**:527–533 DOI 10.2460/ajvr.77.5.527.

Aoun R, Charles I, De Rouen A, Takawira C, Lopez MJ. 2023. Shoe configuration effects on third phalanx and capsule motion of unaffected and laminitic equine hooves *in-situ*. *PLOS ONE* **18(5)**:e0285475 DOI 10.1371/journal.pone.0285475.

Aoun R, Takawira C, Lopez MJ. 2024. Horseshoe effects on equine gait—a systematic scoping review. *Veterinary Surgery* **54(1)**:31–51 DOI 10.1111/vsu.14162.

Back W, Pille F. 2013. The role of the hoof and shoeing. In: Back W, Clayton H, eds. *Equine locomotion*. Cambridge: Elsevier, 147–174.

Barrey E. 1990. Investigation of the vertical hoof force distribution in the equine forelimb with an instrumented horseboot. *Equine Veterinary Journal* **22(S9)**:35–38 DOI 10.1111/j.2042-3306.1990.tb04731.x.

Barrey E. 1999. Methods, applications and limitations of gait analysis in horses. *The Veterinary Journal* **157(1)**:7–22 DOI 10.1053/tvjl.1998.0297.

Biknevicius AR, Mullineaux DR, Clayton HM. 2004. Ground reaction forces and limb function in tölting Icelandic horses. *Equine Veterinary Journal* **36(8)**:743–747 DOI 10.2746/0425164044848190.

Boyer K, Federolf P, Lin C, Nigg B, Andriacchi T. 2012. Kinematic adaptations to a variable stiffness shoe: mechanisms for reducing joint loading. *Journal of Biomechanics* **45(9)**:1619–1624 DOI 10.1016/j.jbiomech.2012.04.010.

Burwell J, Rabinowicz E. 1953. The nature of the coefficient of friction. *Journal of Applied Physics* **24(2)**:136–139 DOI 10.1063/1.1721227.

Butler Jr K. 1985. The prevention of lameness by physiologically-sound horseshoeing. In: *Proceedings of the annual convention of the American Association of Equine Practitioners*.

Chateau H, Holden L, Robin D, Falala S, Pourcelot P, Estoup P, Denoix JM, Crevier-Denoix N. 2010. Biomechanical analysis of hoof landing and stride parameters in harness trotter horses running on different tracks of a sand beach (from wet to dry) and on an asphalt road. *Equine Veterinary Journal* **42**:488–495 DOI 10.1111/j.2042-3306.2010.00277.x.

Clarke EJ, Gillen A, Turlo A, Peffers MJ. 2021. An evaluation of current preventative measures used in equine practice to maintain distal forelimb functionality: a mini review. *Frontiers in Veterinary Science* **8**:758970 DOI 10.3389/fvets.2021.758970.

Clayton HM, Hobbs SJ. 2019. Ground reaction forces: the sine qua non of legged locomotion. *Journal of Equine Veterinary Science* **76**:25–35 DOI 10.1016/j.jevs.2019.02.022.

Crevier-Denoix N, Robin D, Pourcelot P, Falala S, Holden L, Estoup P, Desquilbet L, Denoix JM, Chateau H. 2010. Ground reaction force and kinematic analysis of limb loading on two different beach sand tracks in harness trotters. *Equine Veterinary Journal* **42(S38)**:544–551 DOI 10.1111/j.2042-3306.2010.00202.x.

Dutto DJ, Hoyt DF, Cogger EA, Wickler SJ. 2004. Ground reaction forces in horses trotting up an incline and on the level over a range of speeds. *Journal of Experimental Biology* **207(20)**:3507–3514 DOI 10.1242/jeb.01171.

Eliashar E, McGuigan M, Rogers K, Wilson A. 2002. A comparison of three horseshoeing styles on the kinetics of breakover in sound horses. *Equine Veterinary Journal* **34(2)**:184–190 DOI 10.2746/042516402776767303.

Fajdiga G, Šubic B, Kovačič A. 2021. Bending stiffness of hybrid wood-metal composite beams: an experimentally validated numerical model. *Forests* **12(7)**:918 DOI 10.3390/f12070918.

Goetz T, Comstock C. 1985. The use of adjustable heart bar shoes in the treatment of laminitis in horses. In: *31st annual convention of the American Association of Equine Practitioners*, 605–616.

Gustås P, Johnston C, Drevemo S. 2006. Ground reaction force and hoof deceleration patterns on two different surfaces at the trot. *Equine and Comparative Exercise Physiology* **3(4)**:209–216 DOI 10.1017/S147806150667607X.

Hagen J, Bos R, Brouwer J, Lux S, Jung FT. 2021. Influence of trimming, hoof angle and shoeing on breakover duration in sound horses examined with hoof-mounted inertial sensors. *Veterinary Record* **189(4)**:e450 DOI 10.1002/vetr.450.

Hagen J, Hüppler M, Geiger SM, Mäder D, Häfner FS. 2017. Modifying the height of horseshoes: effects of wedge shoes, studs, and rocker shoes on the phalangeal alignment, pressure distribution, and hoof-ground contact during motion. *Journal of Equine Veterinary Science* **53**:8–18 DOI 10.1016/j.jevs.2017.01.014.

Hagen J, Hüppler M, Häfner F, Geiger S, Mäder D. 2016. Modifying horseshoes in the mediolateral plane: effects of side wedge, wide branch, and unilateral roller shoes on the phalangeal alignment, pressure forces, and the footing pattern. *Journal of Equine Veterinary Science* **37**:77–85 DOI 10.1016/j.jevs.2015.12.001.

Heel MCVV, Weeren PRV, Back W. 2006. Compensation for changes in hoof conformation between shoeing sessions through the adaptation of angular kinematics of the distal segments of the limbs of horses. *American Journal of Veterinary Research* **67(7)**:1199–1203 DOI 10.2460/ajvr.67.7.1199.

Hobbs SJ, Clayton HM. 2013. Sagittal plane ground reaction forces, centre of pressure and centre of mass in trotting horses. *The Veterinary Journal* **198**:e14-e19 DOI 10.1016/j.tvjl.2013.09.027.

Hobbs SJ, Robinson MA, Clayton HM. 2018. A simple method of equine limb force vector analysis and its potential applications. *PeerJ* **6**:e4399 DOI 10.7717/peerj.4399.

Hüppler M, Häfner F, Geiger S, Mäder D, Hagen J. 2016. Modifying the surface of horseshoes: effects of eggbar, heartbar, open toe, and wide toe shoes on the phalangeal alignment, pressure distribution, and the footing pattern. *Journal of Equine Veterinary Science* **37**:86–97 DOI 10.1016/j.jevs.2015.12.009.

Ishihara A, Reed SM, Rajala-Schultz PJ, Robertson JT, Bertone AL. 2009. Use of kinetic gait analysis for detection, quantification, and differentiation of hind limb lameness and spinal ataxia in horses. *Journal of the American Veterinary Medical Association* **234(5)**:644–651 DOI 10.2460/javma.234.5.644.

Kambhampati SB. 2007. Constructing a pedotti diagram using excel charts. *Journal of Biomechanics* **40(16)**:3748–3750 DOI 10.1016/j.jbiomech.2007.06.012.

Karle A, Tank P, Vedpathak H, Mahida H, Shah R, Dhami M. 2010. Horseshoeing: an overview. *Veterinary World* **3(3)**:148–151.

Khumsap S, Clayton H, Lanovaz J, Bouchey M. 2002. Effect of walking velocity on forelimb kinematics and kinetics. *Equine Veterinary Journal* **34(S34)**:325–329 DOI 10.1111/j.2042-3306.2002.tb05441.x.

Lawrence RM. 1898. *The magic of the horse-shoe: with other folk-lore notes*. Valparaiso, Indiana: Obscure Press.

Lewis K, Northrop AJ, Crook GM, Mather J, Martin JH, Holt D, Clayton HM, Roepstorff L, Michael'Mick' LP, Hobbs SJ. 2015. Comparison of equipment used to measure shear properties in equine arena surfaces. *Biosystems Engineering* **137**:43–54 DOI 10.1016/j.biosystemseng.2015.07.006.

Lin S-Y, Su P-F, Chung C-H, Hsia C-C, Chang C-H. 2017. Stiffness effects in rocker-soled shoes: biomechanical implications. *PLOS ONE* **12(1)**:e0169151 DOI 10.1371/journal.pone.0169151.

McLaughlin RM, Gaughan EM, Roush JK, Skaggs CL. 1996. Effects of subject velocity on ground reaction force measurements and stance times in clinically normal horses at the walk and trot. *American Journal of Veterinary Research* **57(1)**:7–11 DOI 10.2460/ajvr.1996.57.01.7.

Moyer W, Anderson J. 1975. Lamenesses caused by improper shoeing. *Journal of the American Veterinary Medical Association* **166(1)**:47–52.

O'Grady SE. 2017. Therapeutic shoes: application of principles. In: Belknap J, Geor R, eds. *Equine laminitis*. Hoboken: JohnWiley & Sons, Inc., 341–353 DOI 10.1002/9781119169239.ch38.

O'Grady S. 2020. The proper application of the wooden shoe: an overview. *Equine Veterinary Education* **32(8)**:415–423 DOI 10.1111/eve.13031.

O'Grady SE, Parks AH. 2008. Farriery options for acute and chronic laminitis. In: *American Association of equine practitioners*.

O'Grady S, Steward M. 2009. The wooden shoe as an option for treating chronic laminitis. *Equine Veterinary Education* **21(2)**:107–112 DOI 10.2746/095777309X397888.

O'Grady SE, Steward ML, Parks AH. 2007. How to construct and apply the wooden shoe for treating three manifestations of chronic laminitis. In: *How to construct and apply the wooden shoe for treating three manifestations of chronic laminitis*, 423–429.

Pardoe C, McGuigan M, Rogers K, Rowe L, Wilson A. 2001. The effect of shoe material on the kinetics and kinematics of foot slip at impact on concrete. *Equine Veterinary Journal* **33(S33)**:70–73 DOI 10.1111/j.2042-3306.2001.tb05363.x.

Parkes RS, Witte TH. 2015. The foot-surface interaction and its impact on musculoskeletal adaptation and injury risk in the horse. *Equine Veterinary Journal* **47(5)**:519–525 DOI 10.1111/evj.12420.

Parks A. 2003. Form and function of the equine digit. *Veterinary Clinics: Equine Practice* **19(2)**:285–307 DOI 10.1016/s0749-0739(03)00018-x.

Parks AH. 2012. Therapeutic farriery: one veterinarian's perspective. *Veterinary Clinics of North America: Equine Practice* **28(2)**:333–350 DOI 10.1016/j.cveq.2012.05.003.

Pereira S, Anand S, Rajendran S, Wood C. 2007. A study of the structure and properties of novel fabrics for knee braces. *Journal of Industrial Textiles* **36(4)**:279–300 DOI 10.1177/1528083707072357.

Robin D, Chateau H, Pacquet L, Falala S, Valette JP, Pourcelot P, Ravary B, Denoix JM, Crevier-Denoix N. 2009. Use of a 3D dynamometric horseshoe to assess the effects of an all-weather waxed track and a crushed sand track at high speed trot: preliminary study. *Equine Veterinary Journal* **41(3)**:253–256 DOI 10.2746/042516409x397965.

Roepstorff L, Johnston C, Drevemo S. 1999. The effect of shoeing on kinetics and kinematics during the stance phase. *Equine Veterinary Journal* **31(30)**:279–285 DOI 10.1111/j.2042-3306.1999.tb05235.x.

Rogers CW, Back W. 2003. Wedge and eggbar shoes change the pressure distribution under the hoof of the forelimb in the square standing horse. *Journal of Equine Veterinary Science* **23(7)**:306–309 DOI 10.1016/S0737-0806(03)01009-8.

Rogers CW, Back W. 2007. The effect of plain, eggbar and 6°-wedge shoes on the distribution of pressure under the hoof of horses at the walk. *New Zealand Veterinary Journal* **55(3)**:120–124 DOI 10.1080/00480169.2007.36753.

Setterbo JJ, Garcia TC, Campbell IP, Reese JL, Morgan JM, Kim SY, Hubbard M, Stover SM. 2009. Hoof accelerations and ground reaction forces of Thoroughbred racehorses measured on dirt, synthetic, and turf track surfaces. *American Journal of Veterinary Research* **70(10)**:1220–1229 DOI 10.2460/ajvr.70.10.1220.

Steward ML. 2003. How to construct and apply atraumatic therapeutic shoes to treat acute or chronic laminitis in the horse. In: *Proceedings of the 49th annual convention of the American Association of Equine Practitioners, New Orleans, Louisiana, USA*.

Teoh JC, Low JH, Lim YB, Shim VP-W, Park J, Park S-B, Park SJ, Lee T. 2013. Investigation of the biomechanical effect of variable stiffness shoe on external knee adduction moment in various dynamic exercises. *Journal of Foot and Ankle Research* **6**:1–9 DOI 10.1186/1757-1146-6-1.

Van Heel M, Moleman M, Barneveld A, Van Weeren P, Back W. 2005. Changes in location of centre of pressure and hoof-unrollment pattern in relation to an 8-week shoeing interval in the horse. *Equine Veterinary Journal* **37(6)**:536–540 DOI 10.2746/042516405775314925.

Van Heel M, VanWeeren P, Back W. 2006. Shoeing sound Warmblood horses with a rolled toe optimises hoof-unrollment and lowers peak loading during breakover. *Equine Veterinary Journal* **38(3)**:258–262 DOI 10.1111/j.2042-3306.2006.tb05549.x.

Wang P, Takawira C, Taguchi T, Niu X, Nazzal MD, Lopez MJ. 2021. Assessment of the effect of horseshoes with and without traction adaptations on the gait kinetics of nonlame horses during a trot on a concrete runway. *American Journal of Veterinary Research* **82(4)**:292–301 DOI 10.2460/ajvr.82.4.292.

Weishaupt MA, Hogg H, Auer J, Wiestner T. 2010. Velocity-dependent changes of time, force and spatial parameters in Warmblood horses walking and trotting on a treadmill. *Equine Veterinary Journal* **42**:530–537 DOI 10.1111/j.2042-3306.2010.00190.x.